

# A synthesis of radial growth patterns preceding tree mortality

MAXIME CAILLERET<sup>1</sup>, STEVEN JANSEN<sup>2</sup>, ELISABETH M. R. ROBERT<sup>3,4,5</sup>, LUCÍA DESOTO<sup>6</sup>, TUOMAS AAKALA<sup>7</sup>, JOSEPH A. ANTOS<sup>8</sup>, BARBARA BEIKIRCHER<sup>9</sup>, CHRISTOF BIGLER<sup>1</sup>, HARALD BUGMANN<sup>1</sup>, MARCO CACCIANIGA<sup>10</sup>, VOJTĚCH ČADA<sup>11</sup>, JESUS J. CAMARERO<sup>12</sup>, PAOLO CHERUBINI<sup>13</sup>, HERVÉ COCHARD<sup>14</sup>, MARIE R. COYEA<sup>15</sup>, KATARINA ČUFAR<sup>16</sup>, ADRIAN J. DAS<sup>17</sup>, HENDRIK DAVI<sup>18</sup>, SYLVAIN DELZON<sup>19</sup>, MICHAEL DORMAN<sup>20</sup>, GUILLERMO GEA-IZQUIERDO<sup>21</sup>, STEN GILLNER<sup>22,23</sup>, LAUREL J. HAAVIK<sup>24,25</sup>, HENRIK HARTMANN<sup>26</sup>, ANA-MARIA HEREŞ<sup>3,27</sup>, KEVIN R. HULTINE<sup>28</sup>, PAVEL JANDA<sup>11</sup>, JEFFREY M. KANE<sup>29</sup>, VYACHESLAV I. KHARUK<sup>30</sup>, THOMAS KITZBERGER<sup>31,32</sup>, TAMIR KLEIN<sup>33</sup>, KOEN KRAMER<sup>34</sup>, FREDERIC LENS<sup>35</sup>, TOM LEVANIC<sup>36</sup>, JUAN C. LINARES CALDERON<sup>37</sup>, FRANCISCO LLORET<sup>3,38</sup>, RAQUEL LOBO-DO-VALE<sup>39</sup>, FABIO LOMBARDI<sup>40</sup>, ROSANA LÓPEZ RODRÍGUEZ<sup>41,42</sup>, HARRI MÄKINEN<sup>43</sup>, STEFAN MAYR<sup>9</sup>, ILONA MÉSZÁROS<sup>44</sup>, JUHA M. METSARANTA<sup>45</sup>, FRANCESCO MINUNNO<sup>7</sup>, WALTER OBERHUBER<sup>9</sup>, ANDREAS PAPADOPOULOS<sup>46</sup>, MIKKO PELTONIEMI<sup>47</sup>, ANY M. PETRITAN<sup>13,48</sup>, BRIGITTE ROHNER<sup>1,13</sup>, GABRIEL SANGÜESA-BARRERA<sup>12</sup>, DIMITRIOS SARRIS<sup>49,50,51</sup>, JEREMY M. SMITH<sup>52</sup>, AMANDA B. STAN<sup>53</sup>, FRANK STERCK<sup>54</sup>, DEJAN B. STOJANOVIĆ<sup>55</sup>, MARIA L. SUAREZ<sup>32</sup>, MIROSLAV SVOBODA<sup>11</sup>, ROBERTO TOGNETTI<sup>56,57</sup>, JOSÉ M. TORRES-RUIZ<sup>19</sup>, VOLODYMYR TROTSIUK<sup>11</sup>, RICARDO VILLALBA<sup>58</sup>, FLOOR VODDE<sup>59</sup>, ALANA R. WESTWOOD<sup>60</sup>, PETER H. WYCKOFF<sup>61</sup>, NIKOLAY ZAFIROV<sup>62</sup> and JORDI MARTÍNEZ-VILALTA<sup>3,38</sup>

<sup>1</sup>Forest Ecology, Department of Environmental Systems Science, Institute of Terrestrial Ecosystems, ETH Zürich, Universitätstrasse 22, 8092 Zürich, Switzerland, <sup>2</sup>Institute of Systematic Botany and Ecology, Ulm University, Albert-Einstein-Allee 11, 89081 Ulm, Germany, <sup>3</sup>CREAF, Campus UAB, 08193 Cerdanyola del Vallès, Spain, <sup>4</sup>Laboratory of Plant Biology and Nature Management (APNA), Vrije Universiteit Brussel, Pleinlaan 2, 1050 Brussels, Belgium, <sup>5</sup>Laboratory of Wood Biology and Xylarium, Royal Museum for Central Africa (RMCA), Leuvensesteenweg 13, 3080 Terouren, Belgium, <sup>6</sup>Department of Life Sciences, Centre for Functional Ecology, University of Coimbra, Calçada Martin de Freitas, 3000-456 Coimbra, Portugal, <sup>7</sup>Department of Forest Sciences, University of Helsinki, P.O. Box 27 (Latokartanonkaari 7), 00014 Helsinki, Finland, <sup>8</sup>Department of Biology, University of Victoria, PO Box 3020, STN CSC, Victoria, BC V8W 3N5, Canada, <sup>9</sup>Institute of Botany, University of Innsbruck, Sternwartestrasse 15, 6020 Innsbruck, Austria, <sup>10</sup>Dipartimento di Bioscienze, Università degli Studi di Milano, Via Giovanni Celoria 26, 20133 Milano, Italy, <sup>11</sup>Faculty of Forestry and Wood Sciences, Czech University of Life Sciences, Kamýcká 961/129, 165 21 Praha 6-Suchbát, Czech Republic, <sup>12</sup>Instituto Pirenaico de Ecología (IPE-CSIC), Avenida Montañana 1005, 50192 Zaragoza, Spain, <sup>13</sup>Swiss Federal Institute for Forest, Snow and Landscape Research – WSL, Zürcherstrasse 111, 8903 Birmensdorf, Switzerland, <sup>14</sup>Unité Mixte de Recherche (UMR) 547 PIAF, Institut National de la Recherche Agronomique (INRA), Université Clermont Auvergne, 63100 Clermont-Ferrand, France, <sup>15</sup>Département des sciences du bois et de la forêt, Centre for Forest Research, Faculté de foresterie, de géographie et de géomatique, Université Laval, 2405 rue de la Terrasse, Québec, QC G1V 0A6, Canada, <sup>16</sup>Biotechnical Faculty, University of Ljubljana, Jamnikarjeva 101, 1000 Ljubljana, Slovenia, <sup>17</sup>U.S. Geological Survey, Western Ecological Research Center, 47050 Generals Highway, Three Rivers, CA 93271, USA, <sup>18</sup>Ecologie des Forest Méditerranéennes (URFM), Institut National de la Recherche Agronomique (INRA), Domaine Saint Paul, Site Agroparc, 84914 Avignon Cedex 9, France, <sup>19</sup>Unité Mixte de Recherche (UMR) 1202 BIOGECO, Institut National de la Recherche Agronomique (INRA), Université de Bordeaux, 33615 Pessac, France, <sup>20</sup>Department of Geography and Environmental Development, Ben-Gurion University of the Negev, 84105 Beer-Sheva, Israel, <sup>21</sup>Centro de Investigación Forestal (CIFOR), Instituto Nacional de Investigación y Tecnología Agraria y Alimentaria (INIA), Carretera La Coruña km 7.5, 28040 Madrid, Spain, <sup>22</sup>Institute of Forest Botany and Forest Zoology, TU Dresden, 01062 Dresden, Germany, <sup>23</sup>Fachgebiet Vegetationstechnik und Pflanzenverwendung, Institut für Landschaftsarchitektur und Umweltplanung, TU Berlin, 10623 Berlin, Germany, <sup>24</sup>Department of Entomology, University of Arkansas, Fayetteville, AR 72701, USA, <sup>25</sup>Department of Ecology and Evolutionary Biology, University of Kansas, 1450 Jayhawk Boulevard, Lawrence, KS 66045, USA, <sup>26</sup>Max-Planck Institute for Biogeochemistry, Hans Knöll Strasse 10, 07745 Jena, Germany, <sup>27</sup>Department of Biogeography and Global Change, National Museum of Natural History (MNCN), Consejo Superior de Investigaciones Científicas (CSIC), C/Serrano 115bis, 28006 Madrid, Spain, <sup>28</sup>Department of Research, Conservation and Collections, Desert Botanical Garden, 1201 N Galvin Parkway, Phoenix, AZ, USA, <sup>29</sup>Department of Forestry and Wildland Resources, Humboldt State University, 1 Harpst Street, Arcata, CA 95521, USA, <sup>30</sup>Siberian Division of the Russian Academy of

Sciences (RAS), Sukachev Institute of Forest, Krasnoyarsk 660036, Russia, <sup>31</sup>Department of Ecology, Universidad Nacional del Comahue, Quintral S/N, Barrio Jardín Botánico, 8400 San Carlos de Bariloche, Río Negro, Argentina, <sup>32</sup>Instituto de Investigaciones de Biodiversidad y Medio Ambiente (INIBOMA), Consejo Nacional de Investigaciones Científicas y Técnicas (CONICET), Quintral 1250, 8400 San Carlos de Bariloche, Río Negro, Argentina, <sup>33</sup>Institute of Soil, Water, and Environmental Sciences, Volcani Center, Agricultural Research Organization (ARO), PO Box 6, 50250 Beit Dagan, Israel, <sup>34</sup>Alterra – Green World Research, Wageningen University, Droevendaalse steeg 1, 6700AA Wageningen, The Netherlands, <sup>35</sup>Naturalis Biodiversity Center, Leiden University, PO Box 9517, 2300RA Leiden, The Netherlands, <sup>36</sup>Department of Yield and Silviculture, Slovenian Forestry Institute, Večna pot 2, 1000 Ljubljana, Slovenia, <sup>37</sup>Department of Physical, Chemical and Natural Systems, Pablo de Olavide University, Carretera de Utrera km 1, 41013 Seville, Spain, <sup>38</sup>Universitat Autònoma de Barcelona, 08193 Cerdanyola del Vallès, Spain, <sup>39</sup>Forest Research Centre, School of Agriculture, University of Lisbon, Tapada da Ajuda, 1349-017 Lisboa, Portugal, <sup>40</sup>Department of Agricultural Science, Mediterranean University of Reggio Calabria, loc. Feo di Vito, 89060 Reggio Calabria, Italy, <sup>41</sup>Forest Genetics and Physiology Research Group, Technical University of Madrid, Calle Ramiro de Maeztu 7, 28040 Madrid, Spain, <sup>42</sup>Hawkesbury Institute for the Environment, University of Western Sydney, Science Road, Richmond, NSW 2753, Australia, <sup>43</sup>Natural Resources Institute Finland (Luke), Viikinkaari 4, 00790 Helsinki, Finland, <sup>44</sup>Department of Botany, Faculty of Science and Technology, University of Debrecen, Egyetem tér 1, 4032 Debrecen, Hungary, <sup>45</sup>Northern Forestry Centre, Canadian Forest Service, Natural Resources Canada, 5320-122nd Street, Edmonton, AB T6H 3S5, Canada, <sup>46</sup>Department of Forestry and Natural Environment Management, Technological Educational Institute (TEI) of Stereas Elladas, Ag Georgiou 1, 36100 Karpenissi, Greece, <sup>47</sup>Natural Resources Institute Finland (Luke), PO Box 18 (Jokiniemenkuja 1), 01301 Vantaa, Finland, <sup>48</sup>National Institute for Research-Development in Forestry “Marin Dracea”, Eroilor 128, 077190 Voluntari, Romania, <sup>49</sup>Faculty of Pure and Applied Sciences, Open University of Cyprus, Latsia, 2252 Nicosia, Cyprus, <sup>50</sup>Department of Biological Sciences, University of Cyprus, PO Box 20537, 1678 Nicosia, Cyprus, <sup>51</sup>Division of Plant Biology, Department of Biology, University of Patras, 26500 Patras, Greece, <sup>52</sup>Department of Geography, University of Colorado, Boulder, CO 80309-0260, USA, <sup>53</sup>Department of Geography, Planning and Recreation, Northern Arizona University, PO Box 15016, Flagstaff, AZ 86011, USA, <sup>54</sup>Forest Ecology and Forest Management Group, Wageningen University, Droevendaalsesteeg 3a, 6708 PB Wageningen, The Netherlands, <sup>55</sup>Institute of Lowland Forestry and Environment, University of Novi Sad, Antona Cehova 13, PO Box 117, 21000 Novi Sad, Serbia, <sup>56</sup>Dipartimenti di Bioscienze e Territorio, Università del Molise, C. da Fonte Lappone, 86090 Pesche, Italy, <sup>57</sup>European Forest Institute (EFI) Project Centre on Mountain Forests (MOUNTFOR), Via E. Mach 1, 38010 San Michele all'Adige, Italy, <sup>58</sup>Laboratorio de Dendrocronología e Historia Ambiental, Instituto Argentino de Nivología, Glaciología y Ciencias Ambientales (IANIGLA), CCT CONICET Mendoza, Av. Ruiz Leal s/n, Parque General San Martín, Mendoza CP 5500, Argentina, <sup>59</sup>Institute of Forestry and Rural Engineering, Estonian University of Life Sciences, Kreutzwaldi 5, 51014 Tartu, Estonia, <sup>60</sup>Boreal Avian Modelling Project, Department of Renewable Resources, University of Alberta, 751 General Services Building, Edmonton, AB T6G 2H1, Canada, <sup>61</sup>University of Minnesota, 600 East 4th Street, Morris, MN 56267, USA, <sup>62</sup>University of Forestry, Kliment Ohridski Street 10, 1756 Sofia, Bulgaria

## Abstract

Tree mortality is a key factor influencing forest functions and dynamics, but our understanding of the mechanisms leading to mortality and the associated changes in tree growth rates are still limited. We compiled a new pan-continental tree-ring width database from sites where both dead and living trees were sampled (2970 dead and 4224 living trees from 190 sites, including 36 species), and compared early and recent growth rates between trees that died and those that survived a given mortality event. We observed a decrease in radial growth before death in ca. 84% of the mortality events. The extent and duration of these reductions were highly variable (1–100 years in 96% of events) due to the complex interactions among study species and the source(s) of mortality. Strong and long-lasting declines were found for gymnosperms, shade- and drought-tolerant species, and trees that died from competition. Angiosperms and trees that died due to biotic attacks (especially bark-beetles) typically showed relatively small and short-term growth reductions. Our analysis did not highlight any universal trade-off between early growth and tree longevity within a species, although this result may also reflect high variability in sampling design among sites. The intersite and interspecific variability in growth patterns before mortality provides valuable information on the nature of the mortality process, which is consistent with our understanding of the physiological mechanisms leading to mortality. Abrupt changes in growth immediately before death can be associated with generalized hydraulic failure and/or bark-beetle attack, while long-term decrease in growth may be associated with a gradual decline in hydraulic performance coupled with depletion in carbon reserves. Our results imply that growth-based mortality algorithms may be a powerful tool for predicting gymnosperm mortality induced by chronic stress, but not necessarily so for angiosperms and in case of intense drought or bark-beetle outbreaks.

**Keywords:** angiosperms, death, drought, growth, gymnosperms, pathogens, ring-width, tree mortality

Received 8 June 2016; revised version received 12 September 2016 and accepted 11 October 2016

## Introduction

Accelerating rates of tree mortality and forest die-off events have been reported worldwide (e.g., van Mantgem *et al.*, 2009; Allen *et al.*, 2010). These trends have been attributed to direct and indirect impacts of drought stress and higher temperatures (e.g., higher competition intensity as a result of growth enhancement in environments limited by low temperature; Luo & Chen, 2015) and are expected to continue as a result of further global warming and drying in many regions (Cook *et al.*, 2014; Allen *et al.*, 2015). Tree mortality has large impacts on both short-term forest functioning (e.g., forest productivity, water and carbon cycles; Anderegg *et al.*, 2016b) and long-term ecosystem dynamics (Franklin *et al.*, 1987; Millar & Stephenson, 2015), yet our physiological understanding of the mechanisms leading to mortality and our ability to predict mortality and its impacts over space and time is still limited (McDowell *et al.*, 2013; Hartmann *et al.*, 2015). As a result, most dynamic vegetation models that aim to project future forest development are still based on simple mortality algorithms despite their high sensitivity to mortality assumptions (Friend *et al.*, 2014; Bircher *et al.*, 2015). In addition, reliable indicators that can be used to predict individual mortality in the field from local to regional scales are lacking (McDowell *et al.*, 2013).

In contrast to most mortality events caused by short-term external disturbances, such as windthrow, fire or flooding, stress-induced mortality is usually preceded by changes in tree function (e.g., hydraulic conductivity, carbon assimilation) and structure (e.g., individual leaf area) (McDowell *et al.*, 2011; Seidl *et al.*, 2011; but see Nesmith *et al.*, 2015 for potential influence of prefire growth on postfire mortality). In this context, focusing on the temporal variations in radial stem growth rates is pertinent as they reflect changes in individual vitality, productivity, and carbon availability (Dobbertin, 2005; Babst *et al.*, 2014; Aguadé *et al.*, 2015). Although the interannual variability in wood growth is primarily driven by cambial phenology and activity (Delpierre *et al.*, 2015; Körner, 2015) – thus by water availability, air temperature, and photoperiod – several studies have shown the utility of radial growth data for predicting tree mortality probability (e.g., Pedersen, 1998; Bigler & Bugmann, 2004; Wunder *et al.*, 2008; Cailleret

*et al.*, 2016). Most studies used ring-width data as they allow for a long-term (i.e., >20 years) retrospective quantification of annual growth for numerous individuals, sites, and species (e.g., Anderegg *et al.*, 2015a). Such data offer the further advantage of combining a large sample size (in contrast to, for example, dendrometers) with an annual temporal resolution that is helpful to estimate the year of tree death and to detect immediate reactions to intense stress such as drought or insect defoliation (Dobbertin, 2005), unlike forest inventories with multiyear remeasurement periods. Moreover, ring-width data are usually available for almost the entire life span of a tree, which is valuable for exploring long-term and delayed effects of stress on mortality (see Bigler *et al.*, 2007) that would not be detected using methods such as carbon flux measurements or remote sensing.

In most studies, dying trees showed lower radial growth rates prior to death than surviving ones (e.g., Pedersen, 1998; Bigler & Bugmann, 2004; Cailleret *et al.*, 2016). Despite this common pattern, a large variety of growth patterns before mortality have been described in the literature from abrupt or gradual growth reductions to increases in growth before death. This variability is likely associated with differences in species' strategies to face environmental stress, and in their carbon allocation patterns related to growth, defense, and storage (Dietze *et al.*, 2014); for example, stress-tolerant species may survive for many years with low growth rates under continuously stressful conditions (e.g., old *Pinus longaeva*), while stress-sensitive species cannot (e.g., *Populus tremuloides*; Ireland *et al.*, 2014). There is also substantial variability at the intraspecific level: Drought-induced mortality events of *Pinus sylvestris* may be preceded by fast declines (Herguido *et al.*, 2016), or by slow and long-lasting growth reductions (Bigler *et al.*, 2006; Hereş *et al.*, 2012).

Growth patterns before death are also influenced by the type, duration, frequency, and intensity of stress factors that predisposed and triggered mortality. For *Picea engelmannii*, dying trees had lower growth rates than surviving trees when mortality was caused by drought (Bigler *et al.*, 2007), while no differences were observed in two pine species when trees died because of bark-beetles (Kane & Kolb, 2010; Ferrenberg *et al.*, 2014; Sangüesa-Barreda *et al.*, 2015). In case of lethal episodic defoliation, tree death can even be preceded by growth increases (e.g., on *Tamarix* spp. in Hultine *et al.*, 2013). Similarly, intraspecific trade-offs between early growth rates (defined as the first 50 years of a

Correspondence: Maxime Cailleret, tel. +41 44 632 52 08, fax +41 44 632 13 58, e-mail: cailleret.maxime@gmail.com

tree's life) and longevity were commonly – but not consistently – observed (Bigler, 2016; but see Ireland *et al.*, 2014), highlighting the potential disadvantage of investment in growth instead of defenses (Herms & Mattson, 1992; Rose *et al.*, 2009).

Considering the multifactorial character of the mortality process (McDowell *et al.*, 2011; Aguadé *et al.*, 2015; Allen *et al.*, 2015; Anderegg *et al.*, 2015b), and the limited number of species and sites analyzed in most earlier studies, we lack a global, comprehensive appraisal of the changes in growth rates before mortality. This is especially relevant to the detection of variations among sources of mortality (e.g., drought, insect outbreak), environmental conditions, and species, and to the simulation of tree mortality using growth-based models (Bircher *et al.*, 2015). Moreover, the available studies applied different methodologies to derive growth–mortality relationships (see Cailleret *et al.*, 2016), which reduces the strength of meta-analyses. Thus, we compiled a new pan-continental tree-ring width database from published and unpublished datasets that include both dead and living trees growing at the same sites. We compare the growth rates between trees that died and those that survived stress events. In particular, we address the following questions: (i) Are there characteristic changes in recent radial growth prior to mortality? (ii) Did dead trees have higher growth rates when they were young than surviving trees? (iii) To what extent are these growth patterns affected by structure–function differences between gymnosperms and angiosperms, and by the shade and/or drought tolerance of a particular species? and (iv) Are these patterns different depending on the main cause of mortality?

We hypothesize, on the one hand, that short-term (i.e., <5 years) or no decline in growth before death will occur in case of severe biotic attack (especially bark-beetles), or in case of drought-induced embolism of xylem conduits that impedes water transport to the canopy and leads to tissue desiccation ('hydraulic failure' hypothesis; McDowell *et al.*, 2011; Rowland *et al.*, 2015). On the other hand, long-term growth reductions (i.e., >20 years) before mortality will be more likely in response to repeated and gradually increasing environmental stress such as shading or parasitism (e.g., mistletoe), where a slow deterioration of the water and carbon economy may lead to tree death because of a lack of nonstructural carbohydrates (NSC) to sustain metabolic processes like respiration or to build defense compounds ('carbon starvation' hypothesis; McDowell *et al.*, 2011; Hartmann, 2015). Accordingly, we expect longer-term growth reductions in shade- and drought-tolerant species than in stress-sensitive ones, and in gymnosperms than in angiosperms, especially due to the wider hydraulic safety margins of conifers (Choat

*et al.*, 2012). We also hypothesize that trees that died during a specific mortality event will show higher juvenile growth rates than surviving trees (Bigler, 2016).

## Materials and methods

### *Tree-ring width database*

We compiled tree-ring width data (RW; mm) from 58 published and unpublished studies dealing with tree growth and mortality and that satisfied the following constraints: (i) Mortality was mainly induced by stress, and not by abrupt abiotic disturbances such as windthrow, fire, or flooding that may kill trees irrespective of their vitality and growth (but see Nesmith *et al.*, 2015); (ii) both dying and surviving trees were growing together at the same site; and (iii) all individual chronologies had been successfully cross-dated. Overall, the dataset analyzed here included 2970 dead and 4224 living trees growing at 190 sites mostly in North America and Europe in the boreal, temperate, and Mediterranean biomes (Fig. 1; Table 1; see details in Appendix S1).

The sampling approach varied widely across studies. Tree-ring data were derived from cores or cross-sections taken at different sampling heights, from the base to eight meters of height. At 30 sites (15.8% of the sites), tree-ring data were only available for the outermost rings (i.e., partial data). Estimates of cambial age and measures of tree diameter at breast height (DBH) at the time of coring were missing for 58 (30.5%) and 21 (11.1%) sites, respectively, which renders these data inappropriate for our analyses. Trees can die during the growing season before ring formation is complete, which induces an incomplete outermost ring. As the precise (intra-annual) timing of tree death was not available, we did not consider the last ring of the dead trees. The year of death was defined as the year of formation of the outermost ring, and considered as a proxy (cf. Bigler & Rigling, 2013). At the site scale, tree mortality could be synchronous (all events occurring in one year), or spread in time over many years (the maximum range being >100 years; Appendix S1).

A total of 36 species were included in the database, which covered several gymnosperm and angiosperm families, although our dataset mainly included gymnosperms (64% of the species and 86% of the sites), with Pinaceae being the most represented family in terms of the number of species and sites sampled, followed by Fagaceae. Species life history strategies were characterized using two sets of shade and drought tolerance indices derived from Niinemets & Valladares (2006) and from the ForClim dynamic vegetation model (Bugmann, 1996; details in Appendix S2). In addition, species structural traits such as wood density (Chave *et al.*, 2009), total and axial parenchyma (Rodríguez-Calcerrada *et al.*, 2015; Morris *et al.*, 2016), Huber value (ratio of conducting xylem area per supported leaf area; Xylem Functional Traits Database; Choat *et al.*, 2012) as well as species' hydraulic safety margin (difference between minimum seasonal water potential measured in the field and the water potential causing 50% loss of xylem conductivity in the stem; Choat *et al.*, 2012) were used to characterize species responses to drought (see Appendix S2).

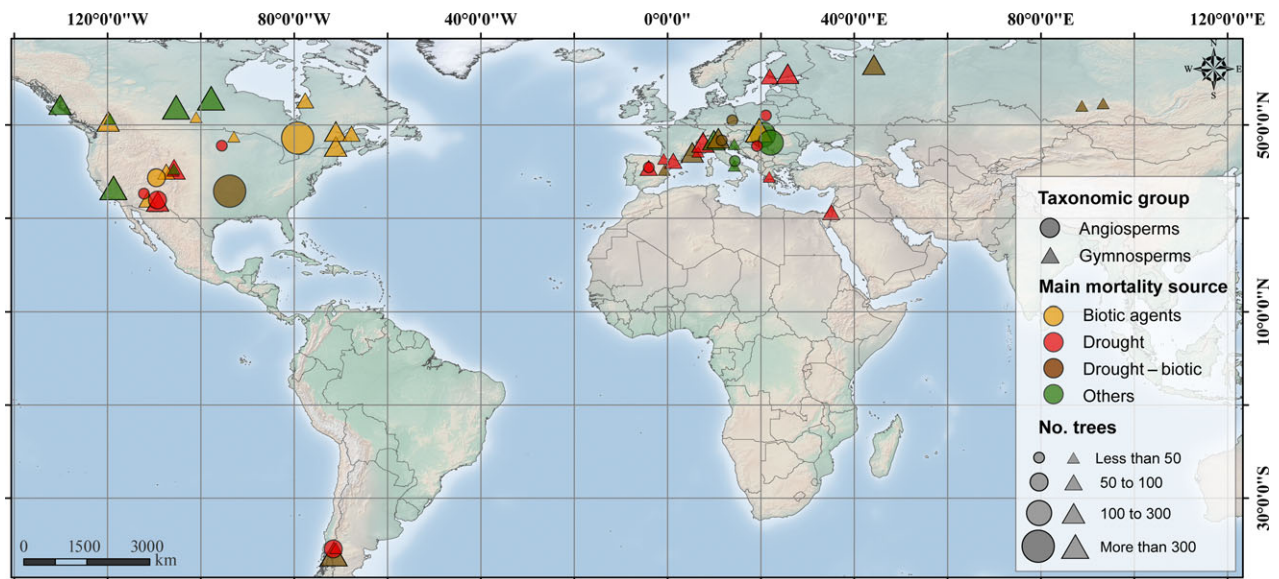


**Fig. 1** Geographic distribution of the sites included in the tree-ring database. Sites with similar species and mortality source in close geographic proximity (difference in latitude and longitude lower than  $1^\circ$ ) were pooled to improve the clarity of the map; thus, the number of symbols does not equal to the number of sites considered here.

**Table 1** Main characteristics of the tree-ring database (ring-width data) compiled from 58 published papers and unpublished data (Appendix S1), showing details about the number of species and sites studied, the number of mortality events, and the number of dying and surviving trees by group of mortality source

		Drought	Drought + biotic	Biotic agents	Others
Species	Angiosperms	6	3	2	3
	Gymnosperms	12	6	9	8
Sites	Angiosperms	10	9	4	4
	Gymnosperms	65	28	43	27
Mortality events	Angiosperms	31	93	25	103
	Gymnosperms	301	252	318	373
Dying trees	Angiosperms	151	160	86	191
	Gymnosperms	564	455	570	793
Surviving trees	Angiosperms	143	565	354	293
	Gymnosperms	646	629	658	936

Note that we also considered 'surviving' information from dying trees (when they were still alive); thus, the number of 'surviving' sets of information is larger than the number of surviving trees.

### *Growth patterns before mortality*

We assumed that all deaths observed for each species within a given site and a given mortality year were consequences of the same mortality process, while deaths that differed in time could be the result of separate processes. Consequently, growth patterns were analyzed for each combination species, site, and mortality year, hereafter referred to as a 'mortality event'. Because of the variable methodologies used across sites, we standardized the data among studies to better detect consistent growth patterns. First, for each mortality event ( $m$ ), we calculated annual growth ratios ( $g_m$ ) between trees that died (dying tree) and conspecific trees that survived that specific mortality event (surviving tree) for their entire life

span up to the mortality year (Berdanier & Clark, 2016; Fig. 2). A  $g_m < 1$  for a given year indicated that dying trees had lower growth rates than surviving ones. Analyzing this variable was useful to quantify relative changes in growth rate over time, which are better linked with mortality probability than absolute growth rates (Das & Stephenson, 2015), but also to remove potential biases due to differences in sampling schemes among studies (Cailleret *et al.*, 2016). Second, to maximize sample size,  $g_m$  were calculated using RW data (1496 mortality events). RW data capture geometric and size effects (Bowman *et al.*, 2013) that must be removed by adequate data standardization. Thus, we only considered surviving trees with a DBH similar to the dying tree measured at a given mortality year ( $\pm 2.5$  cm). In cases where none of the surviving

trees fulfilled this condition, the corresponding mortality event was discarded (123 events were not considered). When not measured in the original study, DBH was estimated as twice the sum of all previous ring-width measurements. Direct age effects were not considered here assuming that senescence only marginally affects tree function (Mencuccini *et al.*, 2014). Finally, to assess the dependency of the results to the growth data used,  $g_m$  values were also calculated using basal area increment (BAI; mm<sup>2</sup>) for trees whose DBH was measured (1000 mortality events).

For each of the  $g_m$  time series, we calculated (i) the growth ratio for the year before death ( $g_{f,m}$ ;  $f$  for final) and (ii) the duration of the continuous period with a  $g_m < 1$  before tree death ( $\Delta t_{g < 1, m}$ ; in case of  $g_{f,m} < 1$ ) or the duration of the continuous period with a  $g_m > 1$  before tree death ( $\Delta t_{g \geq 1, m}$ ; in case of  $g_{f,m} \geq 1$  (cf. Fig. 2).

### Early growth rate

At each site for which tree cambial age was available, and instead of focusing on growth patterns *per se*, we analyzed the ratio in mean RW calculated for the first 50 years of each tree's life between trees that died and trees that survived a given mortality event ( $g_{50,m}$ ). A 50-year period has been used in previous studies linking longevity with growth rates during this period (see Ireland *et al.*, 2014 and Bigler, 2016). To standardize the data and remove age effects, only surviving trees with an age comparable to the dying one were sampled ( $\pm 2$  years). When no surviving tree fulfilled this criterion, the corresponding mortality event was not considered. This approach has the advantage of using the growth information from surviving trees. However, as species-specific relationships between early growth rates and mortality risk can be affected by methodological choices (Bigler, 2016), we also assessed them (i) by varying the number of years used to calculate early mean RW

(Appendix S3), (ii) using different age windows to sample surviving trees corresponding to each dead one (Appendix S4), and (iii) with a method that is more commonly used, that is, by comparing the growth rate and longevity of dead trees only (Appendix S5).

### Designation of the main factors that triggered mortality

The two major sources of mortality were determined for each site based on the expert assessment of the authors of each study, normally combining climatic analyses, growth and mortality data, and the presence/absence of biotic agents. For the present study, we grouped mortality sources into four groups: 'drought', 'biotic', 'drought and biotic', and 'others'. The first group corresponds to drought-induced mortality caused by a single or several drought events without obvious impact of biotic agents. The group 'biotic' includes sites in which mortality was induced primarily by biotic factors, including bark-beetle outbreaks, intense leaf or bud herbivory by insects, and/or fungal infection. In the third group, the impact of biotic agents (including mistletoes and wood-borers) was associated with drought. Finally, the group 'others' included snow break, frost events, high competition intensity, and cases in which mortality was induced by a combination of causes without a clear preponderating factor or, simply, where mortality causes were not specified. The proportion of mortality events was uniformly distributed among these four classes ranging from 31.4% to 22.2% for the groups 'others' and 'drought', respectively (Table 1).

### Statistical analyses

As the frequency distributions of  $g_{f,m}$  and  $g_{50,m}$  were right-skewed and long-tailed, that is, most of the values ranged between 0 and 2 but values exceeding 100 were possible

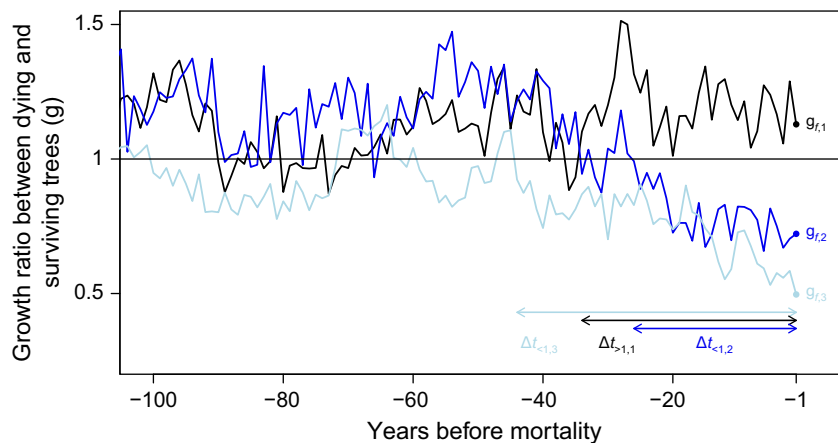


**Fig. 2** Example of time series in growth ratio before mortality (dying/surviving trees) calculated for *Quercus petraea* trees growing at the site 'Runcu' (Romania; A.M. Petritan *et al.* unpublished dataset) for three different mortality events (1: 2009; 2: 2000; and 3: 2010). The duration of the period with reduced or increased growth before death ( $\Delta t_{g < 1, m}$  and  $\Delta t_{g > 1, m}$ , respectively, in arrows), and the growth ratio the year before death ( $g_{f,m}$ ) were used to quantify recent changes in growth rates. [Colour figure can be viewed at [wileyonlinelibrary.com](http://wileyonlinelibrary.com)]

when RW values of living trees  $\sim 0.01$  mm, and as the distribution in  $\Delta t_m$  was not normal, we analyzed median rather than mean values for interpreting 'average' growth patterns. To explore how growth variables differed among species groups (gymnosperms vs. angiosperms) and mortality sources (drought, drought and biotic, biotic, others), we fitted a generalized linear mixed model for  $\Delta t_m$ , and two linear mixed models for  $g_{f,m}$  and  $g_{50,m}$ , considering these categorical components as fixed effects. The variables  $g_{f,m}$  and  $g_{50,m}$  were log-transformed to better satisfy normality of the residuals, and we used a Poisson model with a log-link function for  $\Delta t_m$  as this response variable represents count data (see Bolker *et al.*, 2009). As these variables may change among species and sites irrespective of the fixed effects, random effects were estimated for the intercept with site as grouping factor.

The variation among sites was not examined itself as we lack specific information on their environment (e.g., climate, soil, forest type). However, aggregating the conditional means of the generalized and linear mixed models by species allowed for estimating the variation in growth variables within and among species (e.g., with species drought tolerance) irrespective of their group and of the mortality source. As data on life history and structural traits were not available for every species, these variables were not included as fixed effects in the models to avoid loss of statistical power. Interactions among species groups and mortality sources were not considered in the final models as model fit was reduced in their presence (higher AIC, Akaike Information Criterion). Type-III chi-squares and type-II sum of squares variance analyses were used to estimate the respective impact of species group and source of mortality on  $\Delta t_m$  as well as on  $g_{f,m}$  and  $g_{50,m}$ , respectively. Coefficients of determination were used to assess the percentage contribution of fixed effects alone ( $R^2$  marginal) and both fixed and random effects ( $R^2$  conditional) for explaining the variability in growth patterns (Nakagawa & Schielzeth, 2013).

Finally, resampling procedures were used to assess the dependency of mixed models estimates to the properties of the calibration dataset and to account for the heterogeneity in the number of mortality events per site and per species. For each species, we randomly sampled 21 or 17 mortality events (medians in the database for recent and early growth rates, respectively) with replacement. Depending on the species, the information from a given mortality event could be either replicated (when sample size was low, e.g., for *Nothofagus dombeyi*) or excluded (e.g., for *Quercus rubra*). This sampling procedure was repeated 500 times and mixed-effects models were fitted to each of these 500 datasets. With this approach, each species has the same weight in the calibration dataset and contributes to the same extent to the model estimates. We also generated 500 different datasets with a bootstrap resampling approach. In that case, the number of mortality events was identical to the original dataset but they were randomly selected with replacement, irrespective of the site or species. Mixed models fitting and selection and variance analyses were performed using the packages *lme4*, *lmerTest*, *MuMIn*, and *car* of the open-source software R (R Development Core Team 2015).

## Results

### *Change in growth rates before mortality*

In 83.9% of the mortality events, dying trees showed reduced growth rates prior to death compared with surviving trees ( $g_{f,m} < 1$ ). This reduction was frequently substantial and lasted for many years (Fig. 3a). On average, growth of dying trees in the year before mortality ( $g_{f,m}$ ) was ca. 40% of the growth of surviving trees with a similar DBH (median in RW  $g_{f,m} = 0.42$ ), but  $g_{f,m}$  was highly variable among mortality events (Fig. 4). The distribution of  $g_{f,m}$  was right-skewed with highest frequencies between 0.1 and 0.3 (Fig. 4) and did not significantly change with the approach used to sample surviving trees (Appendix S6). The duration of the period with reduced growth of dying trees ( $\Delta t_{g < 1, m}$ ) was highly variable from 1 to 100 years in 96% of the mortality events, and followed an exponential-like probability density function with a median of 19 years. Around 17% of the mortality events showed a  $\Delta t_{g < 1} \leq 5$  years, and 15% showed a decline period  $> 50$  years. Similar results were obtained using BAI data (Appendix S7), but median values of  $g_{f,m}$  (0.39) and  $\Delta t_{g < 1, m}$  (18 years) were slightly lower than with RW data. Finally, in 241 mortality events (16.1%), dying trees had higher RW than surviving ones the year before death ( $g_{f,m} \geq 1$ ). For these mortality events, the increase in growth was much more recent, as the median of  $\Delta t_{g \geq 1, m}$  was 4 years (Fig. 4).

### *Differences in growth patterns before mortality across species groups and mortality sources*

The variation in  $g_{f,m}$  and  $\Delta t_m$  was high within species groups and mortality groups, with the same order of magnitude as the variation within species and sites (quantile coefficients of dispersion; Appendix S8). As a consequence, the fixed effects considered in the generalized and linear mixed models explained only a small part of the variance in  $g_{f,m}$  and  $\Delta t_m$  ( $R^2$  marginal = 0.06 and 0.03, respectively); however, significant differences among species groups and mortality sources could be detected (Table 2). Intersite variability explained a larger part of the variance ( $R^2$  conditional = 0.18 and 0.26) that could be related to interspecific differences in shade and drought tolerance (within species group). Results of the generalized and linear mixed models were consistent regardless of the data source (RW or BAI data; Appendix S9), regardless of the properties of the calibration dataset in terms of the distribution of mortality events per site and species (Table 2 and Appendix S10), and

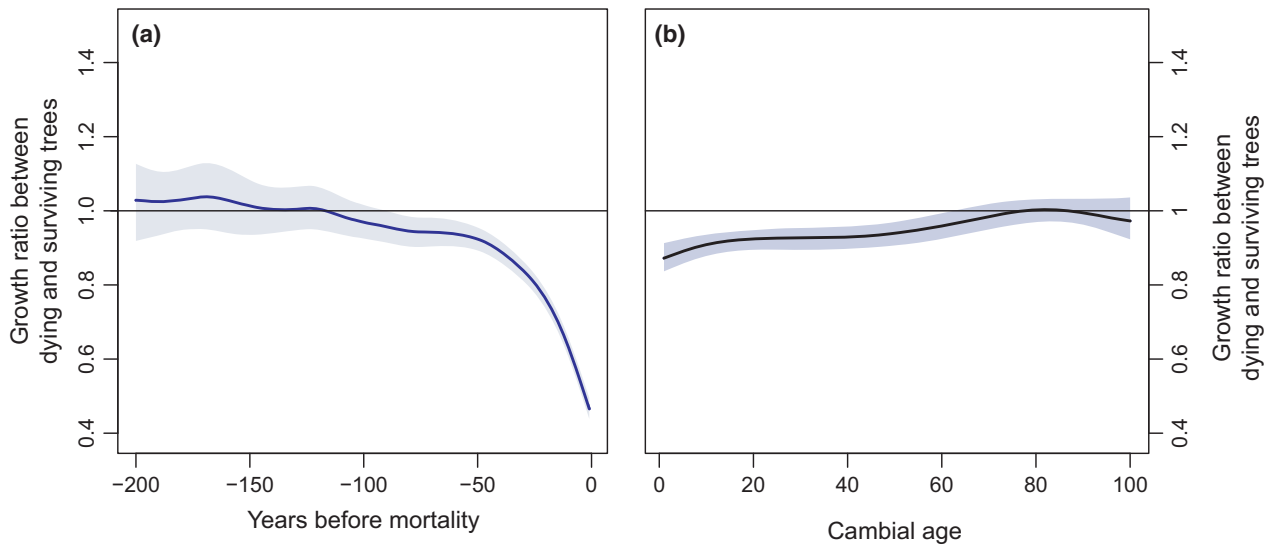


**Fig. 3** (a) Temporal change in growth ratio between dying and surviving trees before mortality and (b) ontogenetic change in growth ratio calculated using ring-width data (RW) and considering all mortality events. Shaded areas represent the 95% confidence intervals of the medians from bootstrapping (1000 resamplings). [Colour figure can be viewed at [wileyonlinelibrary.com](http://wileyonlinelibrary.com)]

regardless of whether dying trees were grouped per mortality year or not (Appendix S11).

In case of drought-induced mortality, the median in RW  $g_{f,m}$  and  $\Delta t_m$  predicted by the mixed-effects models was 0.42 and 19 years, respectively (Fig. 5a), identical to the values obtained when considering all sources of mortality. Relative to cases in which drought was the main source of mortality,  $\Delta t_m$  and  $g_{f,m}$  did not significantly differ when drought was associated with biotic agents. Growth reductions, however, tended to be shorter and more intense (lower  $\Delta t_m$  and higher  $g_{f,m}$ , respectively), when trees were killed by biotic agents alone ( $P < 0.1$ ; Table 2) and, particularly, when trees were attacked by bark-beetles ( $P < 0.05$ ; Appendix S12). Trees that died because of other factors (including interindividual competition) showed the longest and strongest period of reduced growth before death (predicted median in  $\Delta t_m = 24$  years and in  $g_{f,m} = 0.29$ ; Fig. 5a; Table 2).

Considering all sources of mortality, the period with reduced growth was longer and the associated reduction in growth was stronger for gymnosperms than for angiosperms (predicted medians  $\Delta t_m = 22$  and 16 years, and  $g_{f,m} = 0.41$  and 0.53, respectively; Table 2; Fig. 5b) and, to a lower extent, for 'non-*Quercus*' angiosperms relative to *Quercus* species (Appendix S13). Interestingly, this trend occurred whatever the mortality source, as there was no significant interaction between the effects of species group and mortality source (higher AIC of the mixed models when interactions were included).

#### *Species characteristics associated with growth patterns before mortality*

At the species level, long-term reductions in growth (high  $\Delta t_m$ ) were mainly observed for shade-tolerant angiosperms, shade- and drought-tolerant gymnosperms, gymnosperms with low wood density, and species with a low amount of wood parenchyma (especially axial parenchyma for angiosperms; ray parenchyma for gymnosperms) (Table 3a). Results were similar when only drought-induced mortality was considered. In this case, gymnosperms with a low Huber value were also characterized by long-term growth reductions before mortality (Table 3b).

Strong reductions in growth before death (low  $g_{f,m}$ ) were detected for species with a low amount of wood parenchyma, for shade-tolerant angiosperms, and for species with high hydraulic safety margin (Table 3a). In case of drought-induced mortality, gymnosperms with low Huber values had also stronger growth reductions (Table 3b). The relationship between  $g_{f,m}$  and species drought tolerance was inconsistent, as opposite trends were found for gymnosperms and angiosperms and results differed depending on whether the tolerance indices used were derived from Niinemets & Valadares (2006) or from ForClim (Table 3b).

#### *Early growth rates*

Dying trees tended to have lower averaged early growth rate than conspecific surviving ones, especially

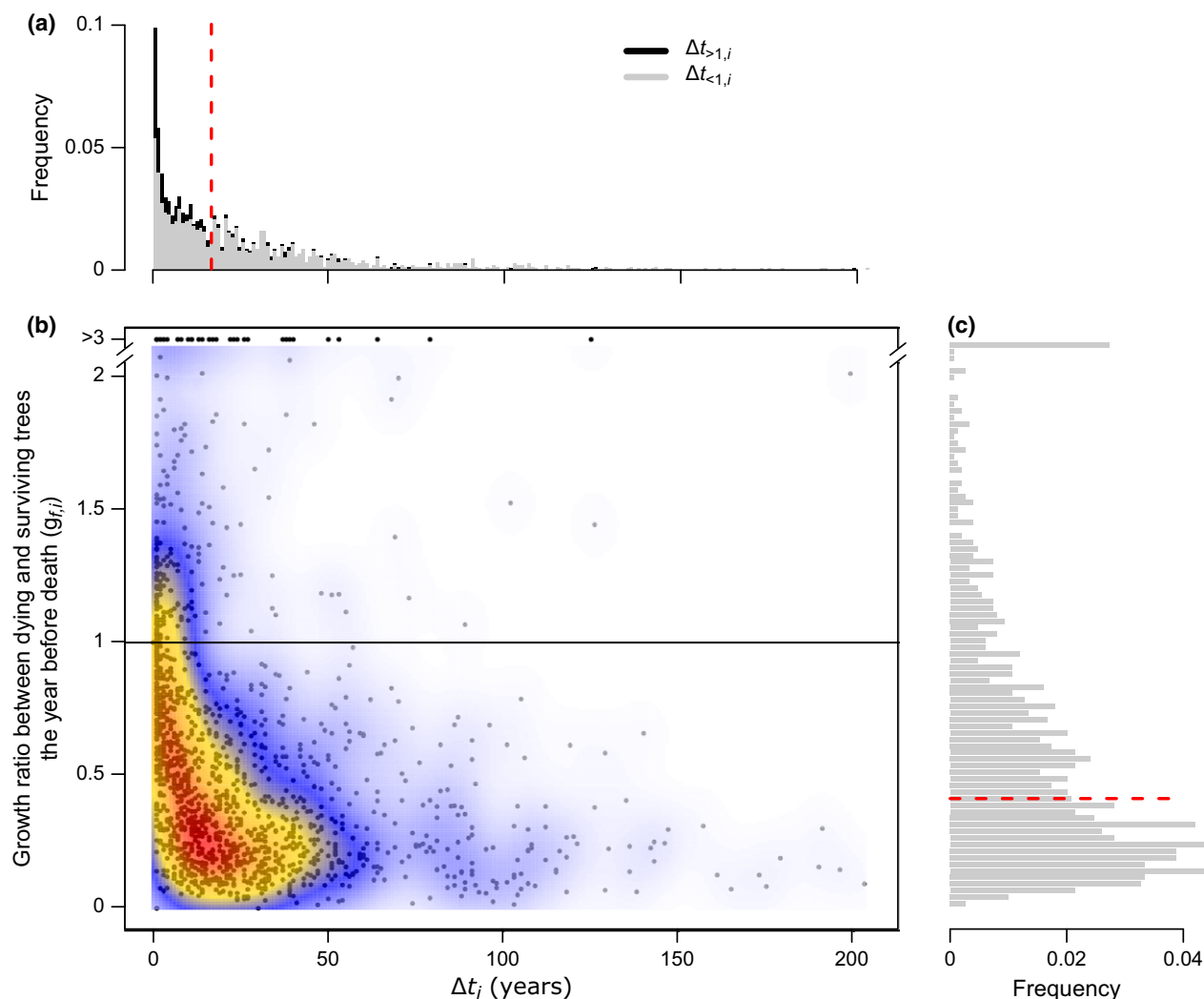


**Fig. 4** Distribution of the duration of the period with reduced or increased growth before death (a;  $\Delta t_{g<1,m}$  and  $\Delta t_{g>1,m}$ , respectively), and the growth ratio the year before death (c;  $g_{f,m}$ ) and both variables (b) calculated using ring-width data. Moving from blue to yellow to red indicates increasing density of mortality events. Red dotted lines plotted on histograms represent median values ( $\Delta t = 17$  years;  $g_f = 0.42$ ).

when a short time period is used to calculate mean juvenile growth rate (Fig. 3b). Considering the first 50 years of a tree's lifetime as representative of its juvenile phase, this trend was observed in 58.6% of the mortality events ( $g_{50,m} < 1$ ; 361/617), but the median in  $g_{50,m}$  was around 0.93 and was not significantly different from one ( $P > 0.1$ ).

Significant differences among mortality groups were highlighted by the generalized linear mixed models. Early growth ratio was highest when mortality was caused by drought alone, and lowest when it was induced by drought combined with biotic agents and by other factors. These differences were significant using  $g_{50,m}$  (Table 2), and also by averaging early growth rate over different time windows (the number

of years fixed across species or as a function of species life span; Appendix S3). There was a tendency toward higher early growth ratio for gymnosperms than for angiosperms, but this result was not consistent when comparing different approaches to define the early growth ratio (Appendix S3).

Considering all sources of mortality,  $g_{50,m}$  showed a negative relationship with species shade tolerance (both species groups; according to ForClim's parameters) and with wood density and the hydraulic safety margin in gymnosperms (Table 3a). The same trends were observed in case of drought-induced mortality, while for angiosperms  $g_{50,m}$  was positively related to their hydraulic safety margin and negatively linked with their wood density (Table 3b).

**Table 2** Summary of the fitted generalized and linear mixed-effects models for the duration of the period with reduced/increased growth before death ( $\Delta t_m$ ), the growth rate of dying trees relative to surviving trees the year before death ( $g_{f,m}$ ), and the growth ratio calculated for the first 50 years of each tree's life ( $g_{50,m}$ )

	Duration of the period with reduced/ increased growth ( $\Delta t_m$ ; chi-sq.) RW, $n = 1496$	Growth ratio the year before death ( $g_{f,m}$ ; sum sq.) log(RW), $n = 1496$	Early growth ratio ( $g_{50,m}$ ; sum sq.) log(RW), $n = 617$
Species group (df = 1)	9.33**	5.60**	0.25 (ns)
Mortality group (df = 3)	9.67*	19.26***	1.58*
Intercept	2.43*** [2.09 to 2.52]	-0.62*** [-0.70 to -0.38]	0.02 (ns) [-0.08 to 0.11]
Gymnosperms	0.57** [0.28 to 0.71]	-0.28** [-0.47 to -0.17]	0.09 (ns) [-0.01 to 0.18]
Drought-Biotic	0.08 (ns) [-0.21 to 0.47]	0.13 (ns) [-0.14 to 0.29]	-0.21** [-0.29 to -0.07]
Biotic agents	-0.30 (*) [-0.51 to 0.10]	0.22* [0.02 to 0.44]	-0.10 (ns) [-0.17 to 0.01]
Others	0.31 (*) [0.00 to 0.68]	-0.28** [-0.53 to -0.09]	-0.21* [-0.36 to -0.06]
$R^2$ marginal	0.03	0.06	0.03
$R^2$ conditional	0.26	0.18	0.22

All variables were calculated using ring-width data (RW). A Poisson model was used for  $\Delta t_m$ , while linear models were fitted to log-transformed  $g_{f,m}$  and  $g_{50,m}$  values.

Top: For  $\Delta t_m$ , chi-square values and significance levels of the chi-square tests of the variable effects are shown, which were derived from type-II variance analysis. Sum of squares and significance levels of the variable effects on  $g_{f,m}$  and  $g_{50,m}$  were calculated using type-III variance analysis.

Center: Estimates of regression coefficients, significance levels (in brackets), and 95% confidence intervals of regression coefficients (in square brackets). The intercept corresponds to the reference species group (angiosperms) and the reference mortality source (drought). Confidence intervals were calculated based on mixed-effects models fitted to 500 different datasets generated using a random sample of 21 or 17 mortality events per species with replacement (medians in the database for recent and early growth ratios, respectively).

Bottom:  $R^2$  marginal and  $R^2$  conditional indicate the variance explained by fixed effects and by both fixed and random effects, respectively.

$n$ , the number of mortality events considered in each model; df, degrees of freedom.

(ns) not significant; (\*)  $P < 0.1$ ; \* $P < 0.05$ ; \*\* $P < 0.01$ ; \*\*\* $P < 0.001$ .

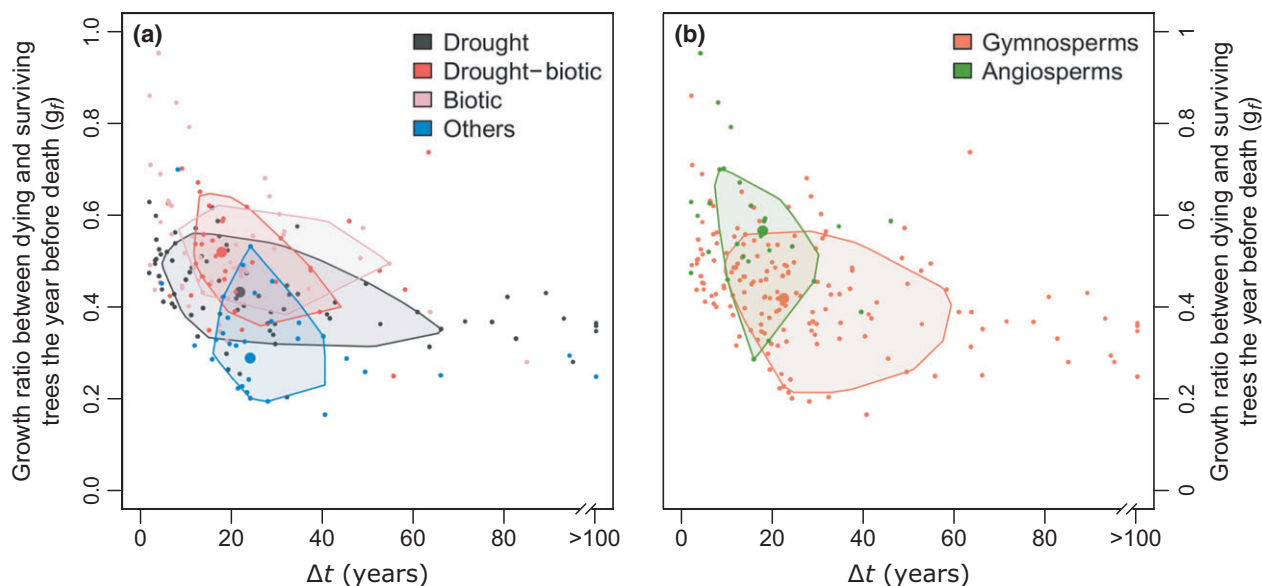


**Fig. 5** Differences in the distribution of the growth ratio the year before death ( $g_f$ ) and the duration of the period with reduced or increased growth ( $\Delta t$ ) predicted by the generalized and linear mixed models among groups of mortality sources (a) and between angiosperms and gymnosperms (b). 50% of the values are included in the convex polygons (bags) whose center (median) is represented by the large dots.

**Table 3** Summary of the relationships between  $\Delta t_m$ ,  $g_{f,m}$  and  $g_{50,m}$  and species characteristics (sign in brackets; adjusted  $R^2$ ; and significance of the relationship) for angiosperms (A.) and gymnosperms (G.)

	no. species		Duration of the period with reduced/increased growth ( $\Delta t_m$ ; RW)		Growth ratio the year before death ( $g_{f,m}$ ; log RW)		no. species		Early growth ratio ( $g_{50,m}$ ; log RW)	
	A.	G.	A.	G.	A.	G.	A.	G.	A.	G.
(a) All mortality sources										
Huber Value	4	10	0.05	-0.01	0.04	<b>(+) 0.03*</b>	2	7	NA	0.01
Hydraulic safety margin	7	12	0.01	-0.01	<b>(-) 0.19*</b>	<b>(-) 0.03*</b>	5	8	-0.08	<b>(-) 0.06*</b>
Wood density	12	20	-0.05	<b>(-) 0.07***</b>	-0.05	-0.01	6	14	0.01	<b>(-) 0.03 (*)</b>
Total parenchyma	7	12	0.02	<b>(-) 0.04*</b>	<b>(+) 0.42**</b>	<b>(+) 0.05**</b>	4	8	0.13	-0.02
Axial parenchyma	7	3	<b>(-) 0.17 (*)</b>	NA	<b>(+) 0.48**</b>	NA	4	8	-0.06	-0.01
DrTol_NV06	10	20	-0.04	-0.01	<b>(+) 0.30**</b>	-0.01	4	13	0.07	-0.01
DrTol_FC	12	15	-0.03	<b>(+) 0.01 (*)</b>	-0.05	-0.01	6	11	-0.08	0.00
ShTol_NV06	10	20	<b>(+) 0.20*</b>	<b>(+) 0.01 (*)</b>	<b>(-) 0.32**</b>	-0.00	4	13	0.01	-0.01
ShTol_FC	12	15	-0.01	<b>(+) 0.02 (*)</b>	<b>(-) 0.28**</b>	-0.00	6	10	<b>(-) 0.21 (*)</b>	<b>(-) 0.06*</b>
(b) Drought-related mortality										
Huber value	3	6	NA	<b>(-) 0.25***</b>	NA	<b>(+) 0.08*</b>	2	4	NA	-0.02
Hydraulic safety margin	5	9	-0.06	-0.00	-0.07	<b>(-) 0.03 (*)</b>	4	7	<b>(+) 0.36*</b>	<b>(-) 0.11*</b>
Wood density	9	12	-0.06	<b>(-) 0.12***</b>	0.05	0.00	4	9	<b>(-) 0.40*</b>	<b>(-) 0.26***</b>
Total parenchyma	5	6	-0.06	<b>(-) 0.29***</b>	0.00	<b>(+) 0.21***</b>	3	4	NA	-0.00
Axial parenchyma	5	3	<b>(-) 0.32*</b>	NA	<b>(+) 0.74***</b>	NA	3	4	NA	<b>(-) 0.18*</b>
DrTol_NV06	7	11	-0.07	-0.01	<b>(+) 0.27*</b>	-0.01	3	8	NA	<b>(-) 0.05 (*)</b>
DrTol_FC	9	8	0.04	<b>(+) 0.15***</b>	0.02	<b>(-) 0.11**</b>	4	6	0.05	-0.02

For each species-specific variable, linear models were fitted to the conditional means (random effect of the site aggregated by species) of the generalized and linear mixed models.  $g_{f,m}$  and  $g_{50,m}$  were log-transformed. Models were not fitted (NA) when data were available for fewer than four species (*no. species*).

The hydraulic safety margin was measured at water potential corresponding to 50% loss of xylem conductivity. Drought and shade tolerance parameters (DrTol and ShTol) were available from Niinemets and Valladares (2006; NV06) and from the ForClim forest model (Bugmann, 1996; FC).

Significant relationships are in boldface. (\*)  $P < 0.1$ ; \* $P < 0.05$ ; \*\* $P < 0.01$ ; \*\*\* $P < 0.001$ . (-): negative relationship; (+): positive relationship.

## Discussion

Based on a new tree-ring width database from temperate, boreal, and Mediterranean forests, our analysis shows that tree mortality is preceded by a growth reduction in ~84% of the mortality events, and supports our initial hypothesis, that is, the decrease in growth before death is most likely stronger and longer for various stress-tolerant gymnosperms than for some angiosperms, and also longer when trees are affected by repeated, mild, but gradually increasing environmental stress such as shading rather than by a severe attack of biotic agents.

### General growth patterns before mortality

Our synthesis supports that dying trees commonly show lower growth rates prior to death than surviving ones ( $g_{f,m} < 1$ ). Considering all mortality events, the decrease in growth the year before death averaged

~60% (median in  $g_{f,m} \sim 0.4$ ). This substantial growth reduction may have been overestimated because of the reduction in the competitive ability of dying trees, which may have benefited the growth of surviving individuals (Cavin *et al.*, 2013). However, this effect was compensated, at least partially, by the fact that the group of 'surviving' trees at a given mortality event may include trees with reduced growth that died shortly after the event. Although growth reductions before mortality are nearly universal, our results show that they can be abrupt or gradual, and the duration of the period with reduced growth ( $\Delta t_m$ ) was highly variable, ranging from 1 to 100 years in 96% of the cases. Overall, 62% of the mortality events showed reduced growth 5–50 years preceding tree death, consistent with previous studies (e.g., ~5 years in Bond-Lamberty *et al.* 2014; 6–12 years in Wyckoff & Clark, 2002; 10–15 years in Ogle *et al.*, 2000; ~15 years in Camarero *et al.*, 2015; ~30 years in Macalady & Bugmann, 2014). These results confirm that trees can survive a long time with

low growth, and emphasize the role of accumulated stress or slow-acting processes (e.g., competition) in tree mortality (Das *et al.*, 2008). However, it is noticeable that in 18% of the mortality events, trees died after a fast ( $\leq 5$  years) growth decline in comparison with trees that survived, highlighting quick tree responses to intense stress. In 19% of the mortality events, trees died after experiencing only a slight decrease or even a short-term increase in growth ( $g_{f,m} > 0.9$ ). Similar observations are rather rare in the literature (but see Ferrenberg *et al.*, 2014; Rowland *et al.*, 2015; Berdanier & Clark, 2016; Herguido *et al.*, 2016) and indicate either that radial growth can be prioritized until the point of death irrespective of environmental stress, or that stress can be strong enough to kill trees without any impact on the carbon budget and its allocation to growth.

In addition to this general pattern, a wide range of growth patterns ( $\Delta t_m$  and  $g_{f,m}$ ) within mortality sources, within species, and within sites was observed. This variability likely reflects (i) the classification of mortality into four broad groups, disregarding the multifactorial character of mortality in many cases and the inherent complexity of mortality processes (Allen *et al.*, 2015; Anderegg *et al.*, 2015b), (ii) the difficult and somewhat arbitrary identification of the sources of mortality and quantification of their respective role under field conditions, and (iii) the high spatiotemporal heterogeneity in microclimate, soil, and stand density conditions and pressure from biotic agents within some sites. Even though most of the variability in  $\Delta t_m$  and  $g_{f,m}$  was not explained by the categorical variables considered here (low variance explained by the generalized and linear mixed models), the high dimensionality of the tree-ring database in terms of sample size, diversity of species, and mortality causes allowed us to detect differences among these groups. Considering that the outputs of the generalized and linear mixed models were coherent no matter what methodology was used to calculate growth ratios (Appendices S6, S9, and S11), and what calibration dataset was used to fit them (Table 2; Appendix S10), we are confident about the reliability of our results.

#### *Growth patterns before mortality vary among sources of mortality*

Although a stronger and longer decrease in growth prior to death could be expected when drought was associated with biotic agents, growth patterns under these conditions were similar to those from trees undergoing drought only. This may be the result of two opposite influences of pathogens on the growth–mortality relationships, depending on their role

within the mortality spiral (predisposing vs. contributing factor; Manion, 1991). On the one hand, a recurrence of moderate biotic attacks (e.g., insect defoliators) and pathogen infection or parasite infestation (e.g., mistletoes or root fungi) reduce carbon, water, and nutrient availability of individual trees, and thus may reduce their growth over both short- and long-term periods and predispose them to subsequent stress factors, and finally to mortality (Schwarze *et al.*, 2003; Hartmann & Messier, 2008; Sangüesa-Barreda *et al.*, 2013; Macalady & Bugmann, 2014; Oliva *et al.*, 2014). On the other hand, massive insect outbreaks may lead to faster tree death that is largely decoupled from growth. Consistent with that interpretation, the decrease in growth before death was shorter and smaller when mortality was related to biotic agents than by drought, and was especially low in case of bark-beetle attacks (contributing factor; Appendix S12).

The slower growth signal associated with mortality induced by bark-beetle outbreaks may reflect a negative effect of carbon allocation to growth rather than defense on tree survival (growth–differentiation balance hypothesis; Herms & Mattson, 1992) and could be explained by several hypotheses. First, the disruptions of carbohydrate transport due to phloem feeding by bark-beetles and xylem occlusion by the fungi they introduce (Hubbard *et al.*, 2013) usually have major consequences for tree functioning, leading to leaf shedding and tree death within a few years (Meddens *et al.*, 2012; Wiley *et al.*, 2016). Second, in the endemic phase, bark-beetles may not preferentially attack trees with slow growth (Sangüesa-Barreda *et al.*, 2015; but see Macalady & Bugmann, 2014), but rather trees with specific size and/or bark thickness, and with lower defense capacities (less resin duct production; Kane & Kolb, 2010; Ferrenberg *et al.*, 2014). Third, considering that tree growth is frequently sink-driven (Körner, 2015), and that defoliation does not increase water stress (but may actually decrease it due to lower whole-tree transpiration), a single biotic defoliation event may not strongly affect tree growth (but see Piper *et al.*, 2015).

Finally, long and strong growth reductions before death were found when mortality was caused by neither drought nor biotic agents, or when the cause was not specified. This group especially included trees that died because of high competition intensity, confirming that shading can suppress trees for a long period before they actually die (Abrams & Orwig, 1996). However, the effects of shading (and competition in general) and other stress factors frequently interact (Myers & Kitajima, 2007; Das *et al.*, 2016) and are difficult to disentangle in field settings.

*Low, short-term growth reductions before death are more common in angiosperms*

As hypothesized, angiosperm species, and especially *Quercus* species, did not commonly show long-lasting reduced growth periods before death but rather died after a fast decline, or even after a short-term increase in growth before death. In contrast, gymnosperm species commonly showed long-term and slow growth reductions before death. Angiosperms tend to recover quickly from extreme events, whereas gymnosperms feature substantial legacy effects (e.g., after drought; Anderegg *et al.*, 2015a), which may reveal the slow but chronic deterioration of their carbon balance and hydraulic performance under gradual or repeated environmental stress (Dickman *et al.*, 2015; Pellizzari *et al.*, 2016). This interpretation is consistent with recent findings showing that reduced NSC concentrations are frequently associated with drought-induced mortality in gymnosperms, but not in angiosperms (Anderegg *et al.*, 2016a). Higher growth fluctuations in angiosperms than in gymnosperms are likely associated with a number of attributes, including (i) high growth efficiency (Brodribb *et al.*, 2012) and productivity in fertile conditions (Augusto *et al.*, 2014), associated with less conservative water use and higher stomatal conductance (Lin *et al.*, 2015); (ii) higher amount of wood parenchyma that may serve to increase storage capacity of NSC and symplastic water (Morris *et al.*, 2016; Plavcová *et al.*, 2016); (iii) high capacity to resprout unlike most species in the Pinaceae family (Zeppel *et al.*, 2015); (iv) narrower hydraulic safety margins (Choat *et al.*, 2012); and possibly, (v) potential capacity to refill embolized xylem conduits (Choat *et al.*, 2012, 2015; but see Mayr *et al.*, 2014 for passive hydraulic recovery in conifers). However, because of the rather small number of angiosperm tree species studied, we acknowledge that more research using a larger number of species, including tropical angiosperms, is needed to validate our hypothesis.

Similarly, growth patterns before death differed among species according to their stress tolerance and resistance and the related structural and functional traits. Because of the relatively low number of the species studied and the limited availability of functional trait data, the correlation among traits was not captured by the univariate analysis we used. Therefore, sufficient care should be taken while interpreting these results. Nevertheless, our findings provide some physiological explanations for the differences between angiosperms and gymnosperms mentioned above. Long-term, strong reductions in growth before death were more frequently observed for drought-tolerant species – according to ForClim's parameters – with wide hydraulic safety margins, a low amount of wood parenchyma,

and low Huber values (for gymnosperms). Shade-tolerant species showed longer and stronger reductions in growth before death than intolerant ones, as evident from comparing species-specific tolerance indices derived from ForClim and Niinemets & Valladares (2006), confirming their ability to survive under shading for a long period (Wyckoff & Clark, 2002; Wunder *et al.*, 2008). Despite the probable link between wood density and mortality risk of angiosperms (Anderegg *et al.*, 2016a), this trait was not associated with particular growth patterns before death.

*No clear intraspecific trade-off between early growth rates and longevity*

Intraspecific trade-offs between growth rates during the juvenile phase and tree longevity have been observed frequently for angiosperm and gymnosperm species, while positive relationships have been rarely found (Black *et al.*, 2008; Ireland *et al.*, 2014; Bigler, 2016). In our synthesis, we did not find evidence of a consistent trade-off in gymnosperms and in angiosperms (Appendix S5). In 58.6% of the mortality events, dying trees had lower early growth rates than surviving ones ( $g_{50,m} < 1$ ), especially when mortality was caused by other agents or by drought and biotic attack than by drought alone. Early investment in rapid growth may provide a strong advantage under light-limited conditions (e.g., in dense stands). However, as highlighted by the high  $g_{50,m}$  values in case of drought-induced mortality and for species with low wood density, it may constitute a disadvantage under dry conditions, where investment into mechanisms to increase water uptake capacity and hydraulic function may be favored. Similarly, promoting early growth instead of whole-tree defenses may be a disadvantage in case of biotic attack or insect defoliation (Rose *et al.*, 2009), but our analysis did not fully support this hypothesis.

As reported by Bigler (2016), methodological aspects related to the experimental design and the sampling strategy may explain differences in the relationship between early growth rates and longevity among sites, species, or studies. In our database, most of the samples did not cover large gradients of early growth and life span (e.g., very old trees or very rapidly/slowly growing trees are missing), mainly because of the relatively low number of dead trees at each site and for each species (Appendix S5). Thus, the lack of consistent trade-off between early growth rates and longevity, and the lack of strong differences among species and mortality sources observed in our synthesis, likely reflects high variability in sampling design among sites and highlights the need for further research on this important topic.

Our results show that radial growth reductions before tree mortality are nearly universal. However, their magnitude and the corresponding growth–mortality relationships varied among sources of mortality, between gymnosperms and angiosperms, and among species. These differences largely support our initial hypothesis: Angiosperms, trees attacked by bark-beetles, or stress-sensitive species (e.g., with narrow hydraulic safety margins) typically show a short-term growth decline prior to mortality, while long-lasting growth reductions tend to occur in gymnosperms, stress-tolerant species and may indicate a long-term (chronic) deterioration of the carbon and water economies. Our analyses show that the temporal changes in growth level before death may provide useful insights into the mechanisms underlying tree mortality, and its complex, multiscale processes. In addition, our results have strong implications for the use of growth data as early warning signal of mortality and for the simulation of tree mortality in dynamic vegetation models. Species- or functional type-specific growth-based mortality algorithms may be powerful for predicting mortality induced by multiannual stress factors and forecasting gymnosperm death. However, for angiosperms and in case of intense drought or bark-beetle outbreaks, growth-based algorithms are unlikely to be predictive, and must be complemented by physiological and/or anatomical information.

### Acknowledgements

This study generated from the COST Action STReESS (FP1106) financially supported by the EU Framework Programme for Research and Innovation HORIZON 2020. We are particularly grateful to Professor Dr. Ute Sass-Klaassen from Wageningen University (the Netherlands), chair of the action, for making this metastudy possible. We also thank members of the Laboratory of Plant Ecology from the University of Ghent (Belgium) for their help while compiling the database; Louise Filion for sharing her dataset; Dario Martin-Benito for providing some ForClim parameters; the ARC-NZ Vegetation Function Network for supporting the compilation of the Xylem Functional Traits dataset; Edurne Martinez del Castillo for the creation of Fig. 1; and two anonymous reviewers and Phillip van Mantgem (USGS) for their suggestions to improve the quality of the manuscript. MC was funded by the Swiss National Science Foundation (Project Number 140968); SJ by the German Research Foundation (JA 2174/3-1); EMRR by the Research Foundation – Flanders (FWO, Belgium), and by the EU HORIZON 2020 Programme through a Marie Skłodowska-Curie IF Fellowship (No. 659191); LDS by a postdoctoral fellowship from the Portuguese Fundação para a Ciência e a Tecnologia (FCT) (SFRH/BPD/70632/2010); TA by the Academy of Finland (Project Nos. 252629 and 276255); JAA by the British Columbia Forest Science Program and the Forest Renewal BC (Canada); BB and WO by the Austrian Science Fund (FWF, Hertha Firnberg Programme Project T667-B16 and FWF P25643-B16); VC, PJ, MS, and VT by the Czech Ministry of Education (MŠMT, Project

COST CZ Nos. LD13064 and LD14074); JJC, JCLC, and GSB by the Spanish Ministry of Economy (Projects CGL2015-69186-C2-1-R, CGL2013-48843-C2-2-R, and CGL2012-32965) and the EU (Project FEDER 0087 TRANSHABITAT); MRC by the Natural Sciences and Engineering Research Council of Canada (NSERC) and by the Service de la protection contre les insectes et les maladies du ministère des forêts du Québec (Canada); KC by the Slovenian Research Agency (ARRS) Program P4-0015; AD by the United States Geological Survey (USGS); HD by the French National Research Agency (ANR, DRYADE Project ANR-06-VULN-004) and the Metaprogram Adaptation of Agriculture and Forests to Climate Change (AAFCC) of the French National Institute for Agricultural Research (INRA); MD by the Israeli Ministry of Agriculture and Rural Development as a chief scientist and by the Jewish National Fund (Israel); GGI by the Spanish Ministry of Economy and Competitiveness (Project AGL2014-61175-JIN); SG by the Bundesministerium für Bildung und Forschung (BMBF) through the Project REGKLAM (Grant Number: 01 LR 0802) (Germany); LJH by the Arkansas Agricultural Experiment Station (United States of America) and the United States Department of Agriculture – Forest Service; HH by the Natural Sciences and Engineering Research Council of Canada; AMH by the Spanish Ministry of Science and Innovation (Projects CGL2007-60120 and CSD2008-0040) and by the Spanish Ministry of Education via a FPU Scholarship; VIK by the Russian Science Foundation (Grant #14-24-00112); TKI and RV by the Consejo Nacional de Investigaciones Científicas y Técnicas (CONICET Grant PIP 112-201101-00058 and PIP 112-2011010-0809) (Argentina); TKI by the Weizmann Institute of Science (Israel) under supervision of Professor Dan Yakir, by the Keren Kayemeth Lelsrael (KKL) – Jewish National Fund (JNF) (Alberta-Israel Program 90-9-608-08), by the Sussman Center (Israel), by the Cathy Wills and Robert Lewis Program in Environmental Science (United Kingdom), by the France-Israel High Council for Research Scientific and Technological Cooperation (Project 3-6735), and by the Minerva Foundation (Germany); KK by the project ‘Resilience of Forests’ of the Ministry of Economic Affairs (the Netherlands – WUR Investment theme KB19); TL by the program and research group P4-0107 Forest Ecology, Biology and Technology (Slovenia); RLV by a postdoctoral fellowship from the Portuguese Fundação para a Ciência e a Tecnologia (FCT; SFRH/BPD/86938/2012); RLR by the EU FP7 Programme through a Marie Skłodowska-Curie IOF Fellowship (No. 624473); HM by the Academy of Finland (Grant Nos. 257641 and 265504); SM by Sparkling Science of the Federal Ministry of Science, Research and Economy (BMWFW) of Austria; IM by the Hungarian Scientific Research Fund (No. K101552); JMM by the Circumpolar-Boreal Alberta grants program from the Natural Science and Engineering Research Council of Canada; MP by the EU Project LIFE12 ENV/FI/000409; AMP by a Swiss Research Fellowship (Sciex-NMSch, Project 13.272 – OAKAGE); JMS by the American National Science Foundation (Grant 0743498); ABS by the British Columbia Ministry of Forests, Lands and Natural Resource Operations (Canada); DS by the Public Enterprise ‘Vojvodinasume’ (project Improvement of Lowland Forest Management); MLS by the Consejo Nacional de Investigaciones Científicas y Técnicas (CONICET Grant PIP 11420110100080) and by El Fondo para la Investigación Científica y Tecnológica (FONCyT Grant PICT 2012-2009); RT by the Italian Ministry of Education (University and Research 2008, Ciclo del Carbonio ed altri gas serra in ecosistemi forestali, naturali ed artificiali dell’America Latina: analisi preliminare, studio di fattibilità e comparazione con ecosistemi italiani) and by the EU LIFE+ Project MANFOR

C.BD. (Environment Policy and Governance 2009, Managing forests for multiple purposes: carbon, biodiversity and socio-economic wellbeing); ARW by the Natural Sciences and Engineering Council (NSERC) (Canada) through the University of Winnipeg and by Manitoba Conservation (Canada); and JMV by the Spanish Ministry of Economy and Competitiveness (Grant CGL2013-46808-R). Any use of trade names is for descriptive purposes only and does not imply endorsement by the U.S. Government.

## References

- Abrams MD, Orwig DA (1996) A 300-year history of disturbance and canopy recruitment of co-occurring white pine and hemlock on the Allegheny Plateau, USA. *Journal of Ecology*, **84**, 353–363.
- Aguadé D, Poyatos R, Gómez M, Oliva J, Martínez-Vilalta J (2015) The role of defoliation and root rot pathogen infection in driving the mode of drought-related physiological decline in Scots pine (*Pinus sylvestris* L.). *Tree Physiology*, **35**, 229–242.
- Allen CD, Macalady AK, Chenchouni H *et al.* (2010) A global overview of drought and heat-induced tree mortality reveals emerging climate change risks for forests. *Forest Ecology and Management*, **259**, 660–684.
- Allen CD, Breshears DD, McDowell NG (2015) On underestimation of global vulnerability to tree mortality and forest die-off from hotter drought in the Anthropocene. *Ecosphere*, **6**, art129.
- Anderegg WRL, Schwalm C, Biondi F *et al.* (2015a) Pervasive drought legacies in forest ecosystems and their implications for carbon cycle models. *Science*, **349**, 528–532.
- Anderegg WRL, Hicke JA, Fisher RA *et al.* (2015b) Tree mortality from drought, insects, and their interactions in a changing climate. *New Phytologist*, **208**, 674–683.
- Anderegg WRL, Klein T, Bartlett M, Sack L, Pellegrini AFA, Choat B, Jansen S (2016a) Meta-analysis reveals that hydraulic traits explain cross-species patterns of drought-induced tree mortality across the globe. *Proceedings of the National Academy of Sciences of the United States of America*, **113**, 5024–5029.
- Anderegg WR, Martínez-Vilalta J, Cailleret M *et al.* (2016b) When a tree dies in the forest: scaling climate-driven tree mortality to ecosystem water and carbon fluxes. *Ecosystems*, **19**, 1133–1147.
- Augusto L, Davies TJ, Delzon S, Schrijver A (2014) The enigma of the rise of angiosperms: can we untie the knot? *Ecology Letters*, **17**, 1326–1338.
- Babst F, Bouriaud O, Papale D *et al.* (2014) Above-ground woody carbon sequestration measured from tree rings is coherent with net ecosystem productivity at five eddy-covariance sites. *New Phytologist*, **201**, 1289–1303.
- Berdanier AB, Clark JS (2016) Multi-year drought-induced morbidity preceding tree death in Southeastern US forests. *Ecological Applications*, **26**, 17–23.
- Bigler C (2016) Trade-offs between growth rate, tree size and lifespan of mountain pine (*Pinus montana*) in the Swiss National Park. *PLoS One*, **11**, e0150402.
- Bigler C, Bugmann H (2004) Predicting the time of tree death using dendrochronological data. *Ecological Applications*, **14**, 902–914.
- Bigler C, Rigling A (2013) Precision and accuracy of tree-ring-based death dates of mountain pines in the Swiss National Park. *Trees*, **27**, 1703–1712.
- Bigler C, Bräker OU, Bugmann H, Dobbertin M, Rigling A (2006) Drought as an inciting mortality factor in Scots pine stands of the Valais, Switzerland. *Ecosystems*, **9**, 330–343.
- Bigler C, Gavin DG, Gunning C, Veblen TT (2007) Drought induces lagged tree mortality in a subalpine forest in the Rocky Mountains. *Oikos*, **116**, 1983–1994.
- Bircher N, Cailleret M, Bugmann H (2015) The agony of choice: different empirical models lead to sharply different future forest dynamics. *Ecological Applications*, **25**, 1303–1318.
- Black BA, Colbert JJ, Pederson N (2008) Relationships between radial growth rates and lifespan within North American tree species. *Ecoscience*, **15**, 349–357.
- Bolker BM, Brooks ME, Clark CJ, Geange SW, Poulsen JR, Stevens MHH, White JSS (2009) Generalized linear mixed models: a practical guide for ecology and evolution. *Trends in Ecology and Evolution*, **24**, 127–135.
- Bond-Lamberty B, Rocha AV, Calvin K, Holmes B, Wang C, Goulden ML (2014) Disturbance legacies and climate jointly drive tree growth and mortality in an intensively studied boreal forest. *Global Change Biology*, **20**, 216–227.
- Bowman DMJS, Brien RJW, Gloor E, Phillips OL, Prior LD (2013) Detecting trends in tree growth: not so simple. *Trends in Plant Science*, **18**, 11–17.
- Brodribb TJ, Bowman DJ, Nichols S, Delzon S, Burrett R (2010) Xylem function and growth rate interact to determine recovery rates after exposure to extreme water deficit. *New Phytologist*, **188**, 533–542.
- Brodribb TJ, Pittermann J, Coomes DA (2012) Elegance versus speed: examining the competition between conifer and angiosperm trees. *International Journal of Plant Sciences*, **173**, 673–694.
- Bugmann HK (1996) A simplified forest model to study species composition along climate gradients. *Ecology*, **77**, 2055–2074.
- Cailleret M, Bigler C, Bugmann H *et al.* (2016) Towards a common methodology for developing logistic tree mortality models based on ring-width data. *Ecological Applications*, **26**, 1827–1841.
- Camarero JJ, Gazol A, Sangüesa-Barreda G, Oliva J, Vicente-Serrano SM (2015) To die or not to die: early warnings of tree dieback in response to a severe drought. *Journal of Ecology*, **103**, 44–57.
- Cavin L, Mountford EP, Peterken GF, Jump AS (2013) Extreme drought alters competitive dominance within and between tree species in a mixed forest stand. *Functional Ecology*, **27**, 1424–1435.
- Chave J, Coomes D, Jansen S, Lewis SL, Swenson NG, Zanne AE (2009) Towards a worldwide wood economics spectrum. *Ecology Letters*, **12**, 351–366.
- Choat B, Jansen S, Brodribb TJ *et al.* (2012) Global convergence in the vulnerability of forests to drought. *Nature*, **491**, 752–755.
- Choat B, Brodersen CR, McElrone AJ (2015) Synchrotron X-ray microtomography of xylem embolism in *Sequoia sempervirens* saplings during cycles of drought and recovery. *New Phytologist*, **205**, 1095–1105.
- Cook BI, Smerdon JE, Seager R, Coats S (2014) Global warming and 21st century drying. *Climate Dynamics*, **43**, 2607–2627.
- Das AJ, Stephenson NL (2015) Improving estimates of tree mortality probability using potential growth rate. *Canadian Journal of Forest Research*, **45**, 920–928.
- Das A, Battles J, van Mantgem PJ, Stephenson NL (2008) Spatial elements of mortality risk in old-growth forests. *Ecology*, **89**, 1744–1756.
- Das AJ, Stephenson NL, Davis KP (2016) Why do trees die? Characterizing the drivers of background tree mortality. *Ecology*, **97**, 2616–2627.
- Delpierre N, Berveiller D, Granda E, Dufrêne E (2015) Wood phenology, not carbon input, controls the interannual variability of wood growth in a temperate oak forest. *New Phytologist*, **210**, 459–470.
- Dickman LT, McDowell NG, Sevanto S, Pangle RE, Pockman WT (2015) Carbohydrate dynamics and mortality in a piñon-juniper woodland under three future precipitation scenarios. *Plant, Cell and Environment*, **38**, 729–739.
- Dietze MC, Sala A, Carbone MS, Czimczik CI, Mantooth JA, Richardson AD, Vargas R (2014) Nonstructural carbon in woody plants. *Annual Review of Plant Biology*, **65**, 667–687.
- Dobbertin M (2005) Tree growth a indicator of tree vitality and of tree reaction to environmental stress: a review. *European Journal of Forest Research*, **124**, 319–333.
- Ferrenberg S, Kane JM, Mitton JB (2014) Resin duct characteristics associated with tree resistance to bark beetles across lodgepole and limber pines. *Oecologia*, **174**, 1283–1292.
- Franklin JF, Shugart HH, Harmon ME (1987) Tree death as an ecological process. *BioScience*, **37**, 550–556.
- Friend AD, Lucht W, Rademacher TT *et al.* (2014) Carbon residence time dominates uncertainty in terrestrial vegetation responses to future climate and atmospheric CO<sub>2</sub>. *Proceedings of the National Academy of Sciences of the United States of America*, **111**, 3280–3285.
- Hartmann H (2015) Carbon starvation during drought-induced tree mortality – are we chasing a myth? *Journal of Plant Hydraulics*, **2**, e005.
- Hartmann H, Messier C (2008) The role of forest tent caterpillar defoliations and partial harvest in the decline and death of sugar maple. *Annals of Botany*, **102**, 377–387.
- Hartmann H, Adams HD, Anderegg WRL, Jansen S, Zeppel MJ (2015) Research frontiers in drought-induced tree mortality: crossing scales and disciplines. *New Phytologist*, **205**, 965–969.
- Hereş AM, Martínez-Vilalta J, López BC (2012) Growth patterns in relation to drought-induced mortality at two Scots pine (*Pinus sylvestris* L.) sites in NE Iberian Peninsula. *Trees*, **26**, 621–630.
- Herguido E, Granda E, Benavides R, García-Cervigón AI, Camarero JJ, Valladares F (2016) Contrasting growth and mortality responses to climate warming of two pine species in a continental Mediterranean ecosystem. *Forest Ecology and Management*, **363**, 149–158.
- Hermis DA, Mattson WJ (1992) The dilemma of plants: to grow or defend. *Quarterly Review of Biology*, **67**, 283–335.
- Hubbard RM, Rhoades CC, Elder K, Negrón J (2013) Changes in transpiration and foliage growth in lodgepole pine trees following mountain pine beetle attack and mechanical girdling. *Forest Ecology and Management*, **289**, 312–317.
- Hultine KR, Dudley TL, Leavitt SW (2013) Herbivory-induced mortality increases with radial growth in an invasive riparian phreatophyte. *Annals of Botany*, **111**, 1197–1206.

- Ireland KB, Moore MM, Fulé PZ, Ziegler TJ, Keane RE (2014) Slow lifelong growth predisposes *Populus tremuloides* trees to mortality. *Oecologia*, **175**, 847–859.
- Kane JM, Kolb TE (2010) Importance of resin ducts in reducing ponderosa pine mortality from bark beetle attack. *Oecologia*, **164**, 601–609.
- Körner C (2015) Paradigm shift in plant growth control. *Current Opinion in Plant Biology*, **25**, 107–114.
- Lin YS, Medlyn BE, Duursma RA *et al.* (2015) Optimal stomatal behaviour around the world. *Nature Climate Change*, **5**, 459–464.
- Luo Y, Chen HY (2015) Climate change-associated tree mortality increases without decreasing water availability. *Ecology Letters*, **18**, 1207–1215.
- Macalady AK, Bugmann H (2014) Growth-mortality relationships in pinon pine (*Pinus edulis*) during severe droughts of the past century: shifting processes in space and time. *PLoS One*, **9**, e92770.
- Manion PD (1991) *Tree Disease Concepts*. Prentice-Hall, Englewood Cliffs, NJ.
- van Mantgem PJ, Stephenson NL, Byrne JC *et al.* (2009) Widespread increase of tree mortality rates in the western United States. *Science*, **323**, 521–524.
- Mayr S, Schmid P, Laur J, Rosner S, Charra-Vaskou K, Dämon B, Hacke UG (2014) Uptake of water via branches helps timberline conifers refill embolized xylem in late winter. *Plant Physiology*, **164**, 1731–1740.
- McDowell NG, Beerling DJ, Breshears DD, Fisher RA, Raffa KF, Stitt M (2011) The interdependence of mechanisms underlying climate-driven vegetation mortality. *Trends in Ecology and Evolution*, **26**, 523–532.
- McDowell NG, Fisher RA, Xu C *et al.* (2013) Evaluating theories of drought-induced vegetation mortality using a multimodel–experiment framework. *New Phytologist*, **200**, 304–321.
- Meddens AJ, Hicke JA, Ferguson CA (2012) Spatiotemporal patterns of observed bark beetle-caused tree mortality in British Columbia and the western United States. *Ecological Applications*, **22**, 1876–1891.
- Mencuccini M, Onate M, Penuelas J, Rico L, Munné-Bosch S (2014) No signs of meristem senescence in old Scots pine. *Journal of Ecology*, **102**, 555–565.
- Millar CI, Stephenson NL (2015) Temperate forest health in an era of emerging megadisturbance. *Science*, **349**, 823–826.
- Morris H, Plavcová L, Cvecko P *et al.* (2016) A global analysis of parenchyma tissue fractions in secondary xylem of seed plants. *New Phytologist*, **209**, 1553–1565.
- Myers JA, Kitajima K (2007) Carbohydrate storage enhances seedling shade and stress tolerance in a neotropical forest. *Journal of Ecology*, **95**, 383–395.
- Nakagawa S, Schielzeth H (2013) A general and simple method for obtaining R<sup>2</sup> from generalized linear mixed-effects models. *Methods in Ecology and Evolution*, **4**, 133–142.
- Nesmith JCB, Das AJ, O'Hara KL, van Mantgem PJ (2015) The influence of prefire tree growth and crown condition on postfire mortality of sugar pine following prescribed fire in Sequoia National Park. *Canadian Journal of Forest Research*, **45**, 910–919.
- Niinemets Ü, Valladares F (2006) Tolerance to shade, drought, and waterlogging of temperate Northern Hemisphere trees and shrubs. *Ecological Monographs*, **76**, 521–547.
- Ogle K, Whitham TG, Cobb NS (2000) Tree-ring variation in pinyon predicts likelihood of death following severe drought. *Ecology*, **81**, 3237–3243.
- Oliva J, Stenlid J, Martínez-Vilalta J (2014) The effect of fungal pathogens on the water and carbon economy of trees: implications for drought-induced mortality. *New Phytologist*, **203**, 1028–1035.
- Pedersen BS (1998) The role of stress in the mortality of midwestern oaks as indicated by growth prior to death. *Ecology*, **79**, 79–93.
- Pellizzari E, Camarero JJ, Gazol A, Sangüesa-Barreda G, Carrer M (2016) Wood anatomy and carbon-isotope discrimination support long-term hydraulic deterioration as a major cause of drought-induced dieback. *Global Change Biology*, **22**, 2125–2137.
- Piper FI, Gundale MJ, Fajardo A (2015) Extreme defoliation reduces tree growth but not C and N storage in a winter-deciduous species. *Annals of Botany*, **115**, 1093–1103.
- Plavcová L, Hoch G, Morris H, Ghiasi S, Jansen S (2016) The amount of parenchyma and living fibres affects storage of non-structural carbohydrates in young stems and roots of temperate trees. *American Journal of Botany*, **103**, 603–612.
- R Core Team (2015) *R: A Language and Environment for Statistical Computing*. R Foundation for Statistical Computing, Vienna, Austria. <http://www.R-project.org/>. (assessed 10 June 2015)
- Rodríguez-Calcerrada J, López R, Salomón R, Gordaliza GG, Valbuena-Carabaña M, Oleksyn J, Gil L (2015) Stem CO<sub>2</sub> efflux in six co-occurring tree species: underlying factors and ecological implications. *Plant, Cell and Environment*, **38**, 1104–1115.
- Rose KE, Atkinson RL, Turnbull LA, Rees M (2009) The costs and benefits of fast living. *Ecology Letters*, **12**, 1379–1384.
- Rowland L, da Costa ACL, Galbraith DR *et al.* (2015) Death from drought in tropical forests is triggered by hydraulics not carbon starvation. *Nature*, **528**, 119–122.
- Sangüesa-Barreda G, Linares JC, Camarero JJ (2013) Drought and mistletoe reduce growth and water-use efficiency of Scots pine. *Forest Ecology and Management*, **296**, 64–73.
- Sangüesa-Barreda G, Linares JC, Camarero JJ (2015) Reduced growth sensitivity to climate in bark-beetle infested Aleppo pines: connecting climatic and biotic drivers of forest dieback. *Forest Ecology and Management*, **357**, 126–137.
- Schwarze FW, Fink S, Deflorio G (2003) Resistance of parenchyma cells in wood to degradation by brown rot fungi. *Mycological Progress*, **2**, 267–274.
- Seidl R, Fernandes PM, Fonseca TF *et al.* (2011) Modelling natural disturbances in forest ecosystems: a review. *Ecological Modelling*, **222**, 903–924.
- Wiley E, Rogers BJ, Hodgkinson R, Landhäusser SM (2016) Nonstructural carbohydrate dynamics of lodgepole pine dying from mountain pine beetle attack. *New Phytologist*, **209**, 550–562.
- Wunder J, Brzeziecki B, Żybura H, Reineking B, Bigler C, Bugmann H (2008) Growth–mortality relationships as indicators of life-history strategies: a comparison of nine tree species in unmanaged European forests. *Oikos*, **117**, 815–828.
- Wyckoff PH, Clark JS (2002) The relationship between growth and mortality for seven co-occurring tree species in the southern Appalachian Mountains. *Journal of Ecology*, **90**, 604–615.
- Zeppel MJ, Harrison SP, Adams HD *et al.* (2015) Drought and resprouting plants. *New Phytologist*, **206**, 583–589.

## Supporting Information

Additional Supporting Information may be found in the online version of this article:

**Appendix S1.** Database built-up.

**Appendix S2.** Species parameters and wood anatomical variables.

**Appendix S3.** Effect of the number of years used to calculate early growth ratio on the estimates of the mixed-effects models fitted to early growth ratio values.

**Appendix S4.** Effect of the age-window used to generate the pair of sample of dead and living trees on the estimates of the mixed-effects models fitted to early growth ratio values.

**Appendix S5.** Relationship between the longevity of dead trees and their mean early growth rate.

**Appendix S6.** Effect of the sampling scheme used to generate the pairs of dying and surviving trees on the  $g_{f,m}$  values.

**Appendix S7.** Temporal change in growth ratio before mortality calculated using ring-width (RW) and basal area increment (BAI) data.

**Appendix S8.** Quartile coefficients of dispersion of  $\Delta t_{m'}$ ,  $g_{f,m'}$  and  $g_{50,m'}$  values.

**Appendix S9.** Summary of the fitted mixed-effects models for  $\Delta t_m$  and  $g_{f,m}$  calculated using both ring-width (RW) and basal area increment (BAI) data.

**Appendix S10.** Summary of the mixed-effects models fitted to datasets derived using a bootstrap approach.

**Appendix S11.** Summary of the fitted mixed-effects models for  $\Delta t_m$ ,  $g_{f,m}$  and  $g_{50,m}$  calculated for each pair of dying tree/surviving trees with a similar DBH.

**Appendix S12.** Summary of the fitted mixed-effects models for  $\Delta t_m$ ,  $g_{f,m}$  and  $g_{50,m}$  for which the class 'biotic agents' was divided into two groups: 'Contributing and inciting' and 'Predisposing' biotic agents.

**Appendix S13.** Summary of the fitted mixed-effects models for  $\Delta t_m$ ,  $g_{f,m}$  and  $g_{50,m}$  for which the class 'angiosperms' was divided into two groups: 'Quercus' and 'non-Quercus' species.